Helical Flow Component of Left Ventricular Assist Devices (LVADs) Outflow Improves Aortic Hemodynamic States

Authors' Contribution:
Study Design A
Data Collection B
Statistical Analysis C
Data Interpretation D
Manuscript Preparation E
Literature Search F
Funds Collection G

BDE   Qi Zhang
ABDEFG   Bin Gao
FG   Yu Chang

School of Life Sciences and Bioengineering, Beijing University of Technology, Beijing, P.R. China

Background: Although LVADs are confirmed to have strong effects on aortic hemodynamics, the precise mechanisms of the helical flow component of LVAD outflow are still unclear.

Material/Methods: To clarify these effects, 3 cases – normal case, flat flow case, and realistic flow case – were designed and studied by using the CFD approach. The normal case denoted the normal aorta without LVAD support, and the flat flow case represented the aorta with the outflow cannula. Similarly, the realistic flow case included the aortic model, the model of outflow cannula, and the model of LVAD. The velocity vector, blood streamline, distribution of wall shear stress (WSS), and the local normalized helicity (LNH) were calculated.

Results: The results showed that the helical component of LVAD outflow significantly improved the aortic hemodynamics. Compared with the flat flow case, the helical flow eliminated the vortex near the outer wall of the aorta and improved the blood flow transport (normal case 0.1 m/s *vs.* flat flow case 0.14 m/s *vs.* realistic flow case 0.30 m/s) at the descending aorta. Moreover, the helical flow was confirmed to even the distribution of WSS, reduce the peak value of WSS (normal case 0.92 Pa *vs.* flat flow case 7.39 Pa *vs.* realistic flow case 5.2Pa), and maintain a more orderly WSS direction.

Conclusions: The helical flow component of LVAD outflow has significant advantages for improving aortic hemodynamic stability. Our study provides novel insights into LVAD optimization.

MeSH Keywords: Finite Element Analysis • Heart, Artificial • Hemodynamics

Full-text PDF: https://www.medscimonit.com/abstract/index/idArt/905940

📄 3887   🖼 —   📊 9   📚 34

LAB/IN VITRO RESEARCH

Background

Left ventricular assist devices (LVADs) have been widely used in the treatment of advanced heart failure patients [1]. It has been confirmed that the implantable devices can meet the physiological requirements of the human body, both at exercise and at rest [2], and their use can reduce mortality and improve quality of life [3]. Along with the development of LVADs, its effects on the aortic hemodynamics have attracted much more attention. For instance, Karmonik et al. reported the effects of LVADs outflow cannular location on the aortic hemodynamic environment by using CFD [4], finding that the anterior geometry achieved lower stress and wall shear stress (WSS) than lateral geometry. Karmonik et al. studied the differences in aortic hemodynamic environment caused by pulsatile and continuous flow LVADs [5]. Reduced pressure and lower WSS in the ascending aorta were observed under pulsatile flow LVADs versus continuous flow LVADs. Caruso et al. reported that the height of the anastomosis could change the aortic hemodynamic states [6], and the outflow graft, placed 2 cm above the ST junction, achieved the most favorable hemodynamic states. Similarly, Yang et al. demonstrated that a large increase in wall shear stress is found near the cannular during LVAD support [7]. Zhang et al. found that the local hemodynamic changes, caused by the outflow cannula location of LVAD, regulated thrombi distribution in the aorta [8]. Currently, our group demonstrated that the LVADs, under pulsatile support mode, could provide significant benefit for preventing atherosclerosis lesions and aortic remodeling [9].

Helical flow is considered an important flow pattern in the aorta [10], as the human aortic arch is curved and twisted to a non-planar geometry [11]. Helical flow is regarded as the rotational motion of blood flow during its passage through the artery [12]. Helical flow has significant physiological benefits for the human body. For instance, Frazin reported that helical flow accounts for a significant amount of normal organ perfusion [13]. Helical blood flow was also confirmed to even the distribution of the aortic wall shear stress and inhibit blood flow stagnation [14].

Although studies were confirmed that LVADs can achieve significant effects on aortic hemodynamic states, and helical flow significantly benefits the cardiovascular system, the LVAD outflow pattern has been assumed to be a flat flow pattern. In our previous study [15], we found significant helical flow components in the LVAD outflow pattern. However, its effects on the aortic hemodynamic states were still unclear.

To clarify the effects of helical flow components of LVAD outflow on aortic hemodynamic states, we performed the present comparative study. We designed 3 cases: a normal aorta (normal case), an aorta supported with flat flow pattern (flat flow case), and an aorta supported with realistic flow pattern (realistic flow case). The flow pattern, distribution of local normalized helicity (LNH), wall shear stress (WSS), and the blood vorticity percentage distribution were calculated to reflect the hemodynamic changes between varied cases.

Material and Methods

Aortic model generation

In this study, 3 geometric models – normal case, flat flow case, and realistic flow case – were established based on the computed tomography angiography (CTA) data, which was obtained from an advanced heart failure patient. The informed consent was signed by the patient for using medical images in the study. The 3D aortic geometric model was reconstructed according to the CTA data, and then we used 3D reconstruction package MIMICS (Materialise, Belgium) to generate the stereolithographic files (STL format). Subsequently, the model was smoothed by using Geomagic (Geomagic, USA) to obtain better surface quality (Figure 1A).

Outflow cannular diameter was set at 12 mm, according to the size of the LVADs outlet. The outflow cannula, assumed as a rigid cannula, was connected at the anterior ascending aortic wall (Figure 1B) by using FreeForm (Geomagic, USA), a commercial software package.

The LVAD, named as BJUT-I VAD, was previously designed by our group [16]. It consists of the housing, anterior blade, impeller, and the rear blade (Figure 1D). The diameter of the housing is 12 mm, and its length is 78 mm. The gap between the impeller and the housing is 0.1 mm. BJUT-I VAD was connected to the ascending aorta by using outflow cannula (Figure 1C). The geometric model of BJUT-I VAD was connected with the aortic model using the FreeForm package (Geomagic, USA) (Figure 1C).

Meshing generation

The grids of the 3 models were generated by utilizing the package Hexpress (Numeca, Belgium), which generates the unstructured hexahedron grids for complex geometric modeling. To determine the appropriate mesh dimension, the grid independency tests, in which the percentage of the distribution of the blood vorticity in the whole aorta was chosen as the criterion, were conducted. According to the results of the test, 24 million hexahedral elements (LVADs 23 million elements, aorta 0.69 million elements) were sufficient for this study (Figure 2A, 2B); the minimum size of the element was 3.232e-12 m^3. To obtain accurate flow pattern near the aortic vessel, 8 boundary layers were generated (Figure 2C). The mesh inside of BJUT-I VAD is shown in the Figure 2D and 2E.
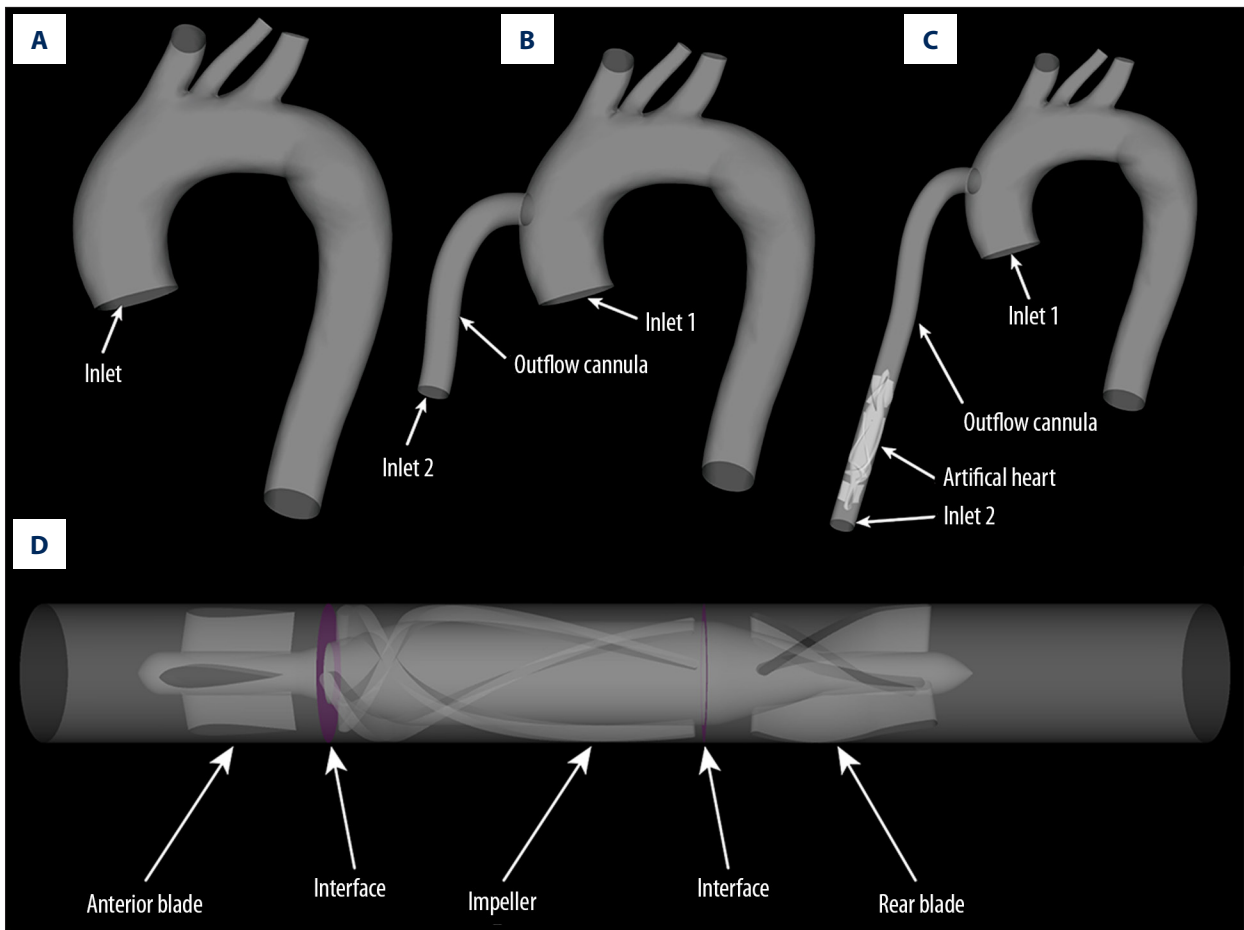
Figure 1. The geometric models used in this study. (**A**) Is the geometric model of normal aorta. (**B**) Is the aortic geometric model supported by flat flow pattern. (**C**) Is the geometric model supported by realistic flow pattern. (**D**) Is the geometric model of LVAD used in this study.

Numerical approaches

The continuity equation and Reynolds averaged Navier–Stokes (RANS) equations were used to describe 3D incompressible flow [17]. The RANS equations were solved by using NUMECA FINE/OPEN 6.1 (Numeca, Belgium), utilizing "Frozen Rotor" approach, finite volume-based pressure-correction algorithm, and a second-order up-winding scheme for the convective derivatives. In this numerical study, the elastic property of the aortic vessel was neglected, which means the deformation of the aortic vessel was not considered. The velocity of the blood, which was connected with the aortic wall, was assumed to be zero (no-slip condition) in this study.

Based on the geometric size of the model, the blood density and the blood flow velocity, the Reynolds number (Re) in the BJUT-I VAD was larger than 5000, while that in the aorta was only less than 900. Hence, the turbulence model was necessary to illustrate the inner flow pattern of LVAD. According to literatures, the k-w SST turbulence model, approved to be

appropriate for calculating the turbulence flow pattern in series type LVAD and aorta, was used. Details of the k-w SST turbulence model and justifications of using it for aortic flow were reported [18]. The inlet turbulence intensity of the aorta was set to be 1.5% for 3 cases to maintain the condition of calculation being same with each other [19].

Calculation settings

In this study, the density and viscosity of blood was set as 1050 kg/m^3 and 0.0035 Pa·s, respectively. The aortic wall was assumed to be no-slip rigid wall. The simulation was conducted under static-state flow conditions. For normal case, the static flow rate 5 L/min was imposed at the aortic root as the inlet boundary condition (Figure 1A inlet). For flat flow case, the static flow rate 1L/min was imposed at the aortic root (Figure 1B inlet 1) and the static flow rate 4 L/min (flat flow pattern) was imposed at the inlet of outflow cannula (Figure 1B inlet 2), according to clinical practice. Similarly, for realistic flow case, the static flow rate 1 L/min was imposed
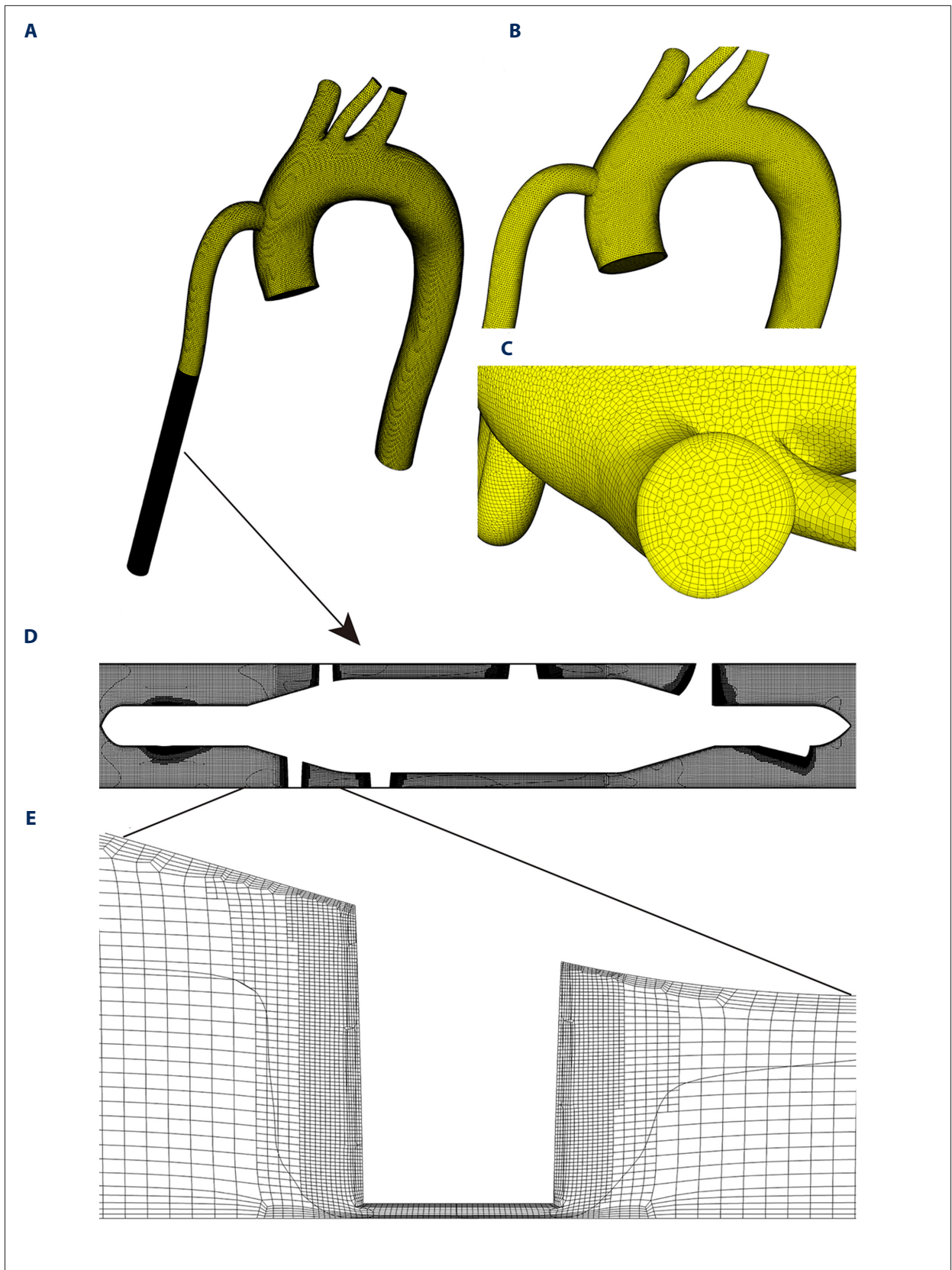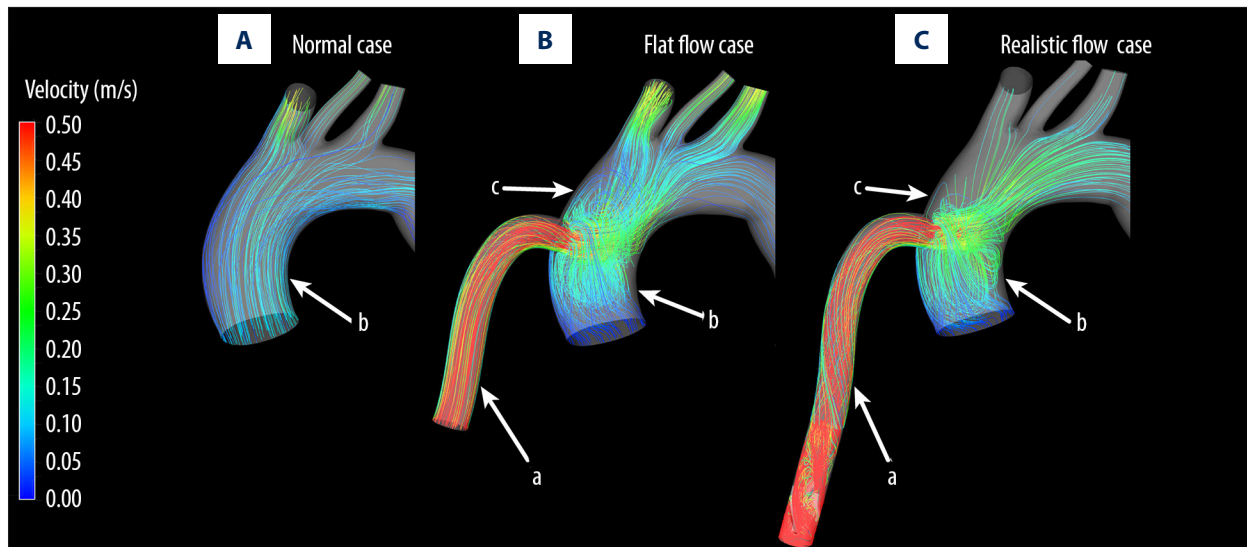
Figure 2. (**A–D**) The mesh of the geometric model.

Figure 3. The streamline of blood in the aorta under 3 cases. (**A**) illustrate the blood streamline under normal case. (**B**) shows the blood streamline under the flat flow case. (**C**) illustrates the blood flow streamline under realistic flow case.

at the aortic root (Figure 1B inlet 1) and the static flow rate 4 L/min (flat flow pattern) was used as the inlet boundary condition (Figure 1B inlet 2), according to the clinical practice. In addition, the LVAD rotational speed was set to be 9000 RPM counter-clockwise to mimic the rotational behavior of the impeller. The zero-pressure boundary conditions were imposed at all of outlets of the model for the 3 cases. The convergence criterion in this study was set as 10^{-3}.

Hemodynamic analysis

The hemodynamic changes between the 3 cases, the flow pattern, wall shear stress (WSS), and local normalized helicity (LNH) were calculated.

WSS was calculated as a function of time during the cycle at each location, which was closed to the wall according to the defining relationship [20], as the equation (1):

$$\overrightarrow{\tau_\omega} = \mu \frac{\Delta \vec{v}}{\Delta \vec{r}} \qquad (1)$$

Where $\overrightarrow{\tau_\omega}$ denoted the wall shear stress, μ represented the absolute viscosity, $\vec{v}$ was the velocity parallel to the wall, and the r was the radial distance from the wall.

The rotating direction of blood flow was confirmed to have strong relationship with the occurrence of vascular disease [21]. The localized normalized helicity (LNH) [22] was proposed to evaluate this characteristic, shown as the equation (2):

$$\text{LNH}(s;t) = \frac{V(s;t) \cdot \omega(s;t)}{|V(s;t)||\omega(s;t)|}, -1 \le LNH \le 1 \qquad (2)$$

Where $\vec{v}$ was the velocity vector, represented the vorticity vector, **s** denoted the position, and t denote the time instant. The LNH value ranged from −1 to +1. −1 shows that the left-handed helical blood flow was dominant, while +1 shows that the right-handed helical blood flow was dominant.

Results

To evaluate the difference of aortic hemodynamic environment between the 3 cases, the blood flow pattern in the aorta, distribution of the WSS, and the distribution of LNH are shown from **Figures 3–9**.

The aortic blood flow pattern

Figure 3 shows the aortic blood flow streamline under 3 cases. Figure 3A is the aortic blood flow streamline under the normal case. Figure 3B shows the aortic blood flow streamline under the flat flow case. Figure 3C illustrates the aortic flow streamline under the realistic flow case. It was seen that the blood flow in the LVAD outflow cannula under realistic flow case contained an obvious helical flow component (region a), while that was not seen under the flat flow case, which was consistent with our previous study [15]. Moreover, compared with the normal case, obvious turbulence flow was seen under both flat flow case and realistic flow case (region b). In addition, 2 vortexes were seen near the graft location of the LVAD outflow cannula under the flat flow case (region c). However, under realistic flow case, 1 of them was significantly weaken by the helical LVAD outflow.
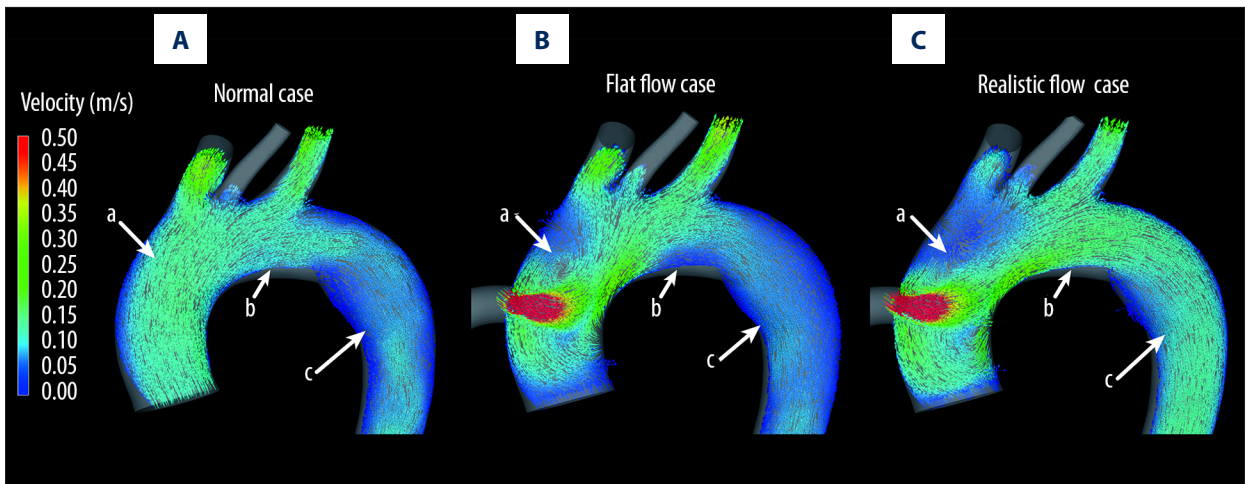
Figure 4. The blood velocity vector in the aorta. (**A**) is the blood velocity vector under the normal case. (**B**) shows the blood velocity vector under the flat flow case. (**C**) illustrates the blood velocity vector under the realistic flow case.
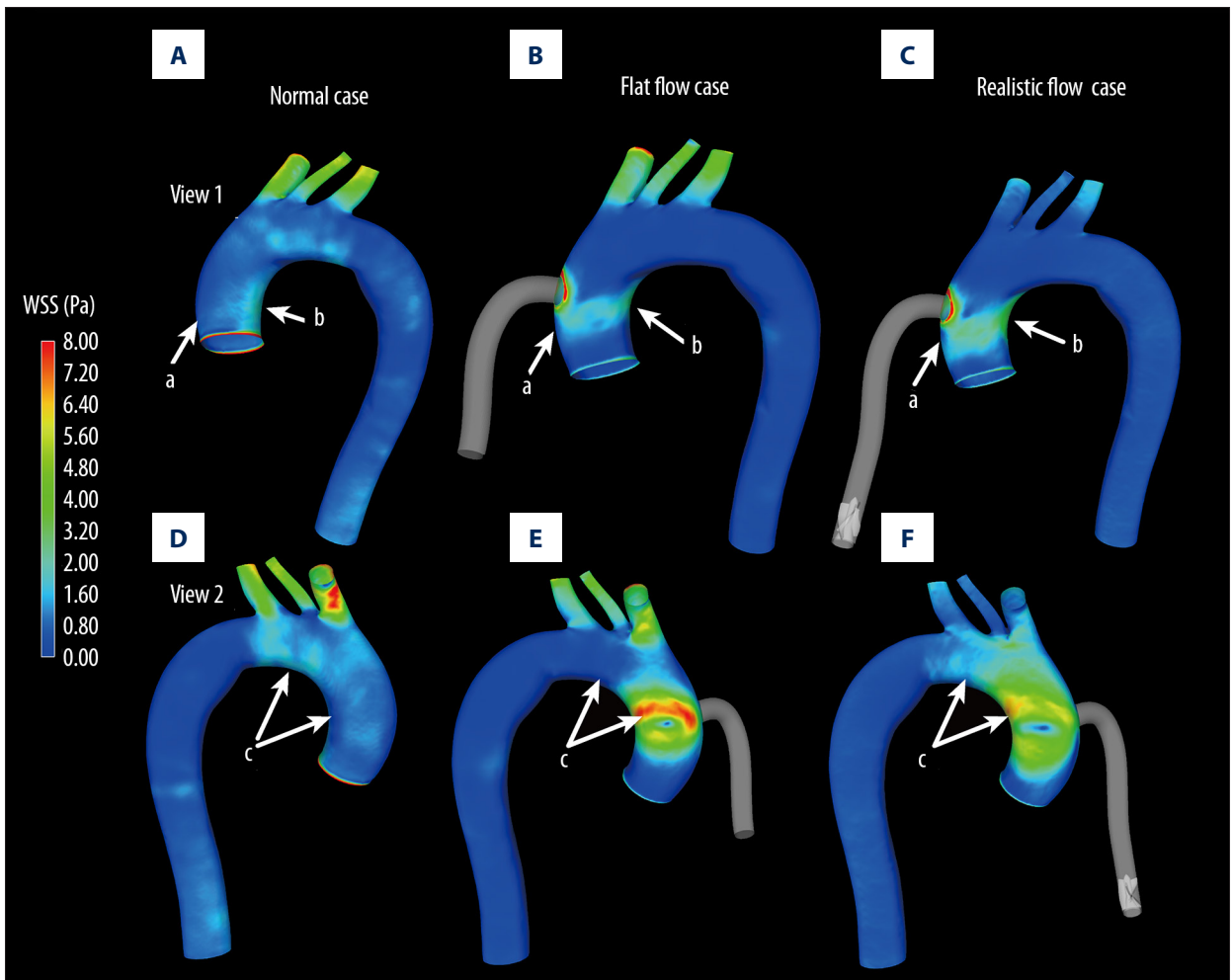

Figure 5. The distribution of WSS under 3 cases. (**A, D**) are the distribution of WSS under normal case. (**B, E**) show the distribution of WSS under flat flow case. (**C, F**) illustrates the distribution of WSS under realistic flow case.
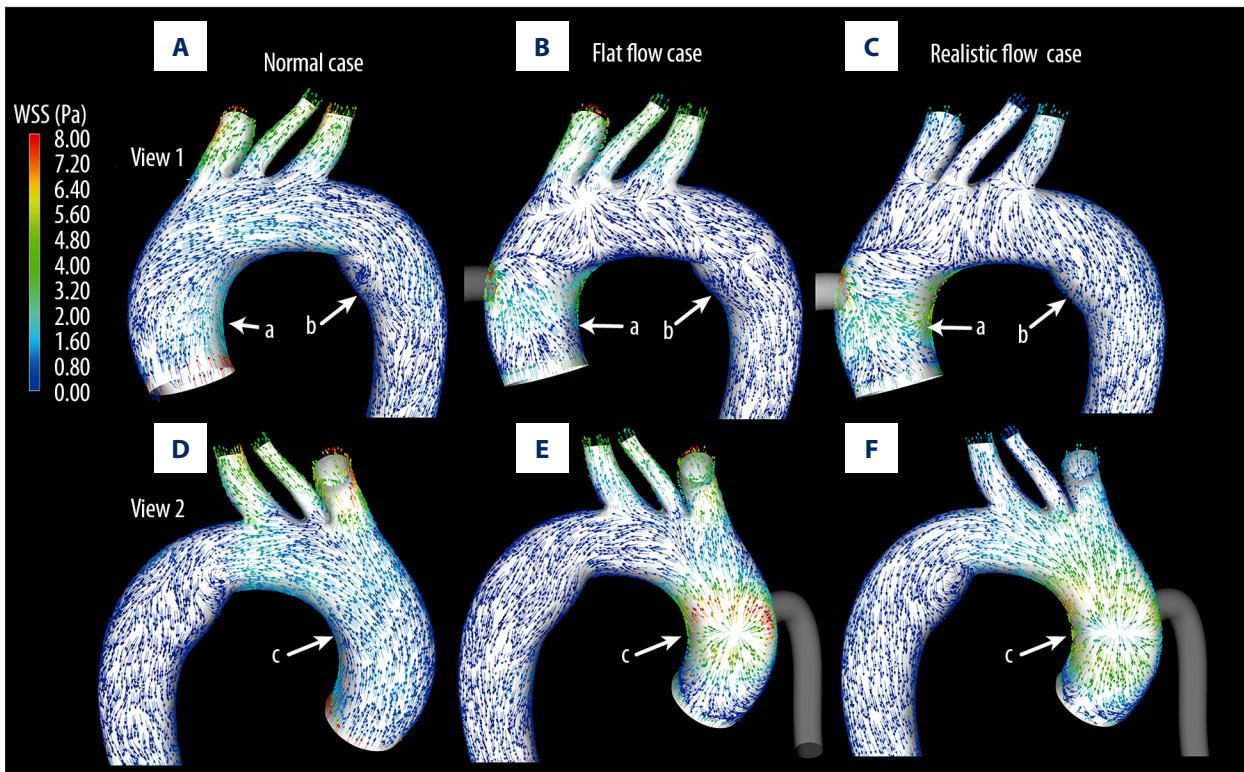
Figure 6. The distribution of WSS vector in the 3 cases. (**A, D**) are the WSS vector distribution in the normal case. (**B, E**) show the WSS vector in the flat flow case. (**C, F**) illustrate the WSS vector in the realistic flow case.
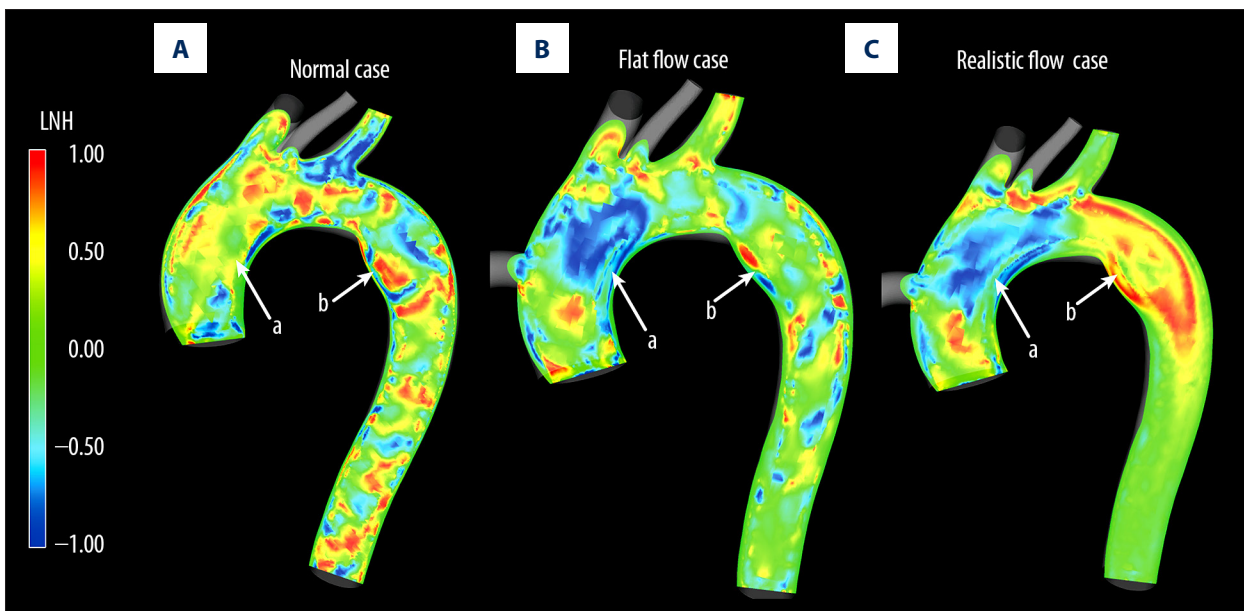

Figure 7. The distribution of LNH under 3 cases. (**A**) shows the distribution of LNH under normal case. (**B**) shows the distribution of LNH under flat flow case. (**C**) illustrates the distribution of LNH under realistic flow case.
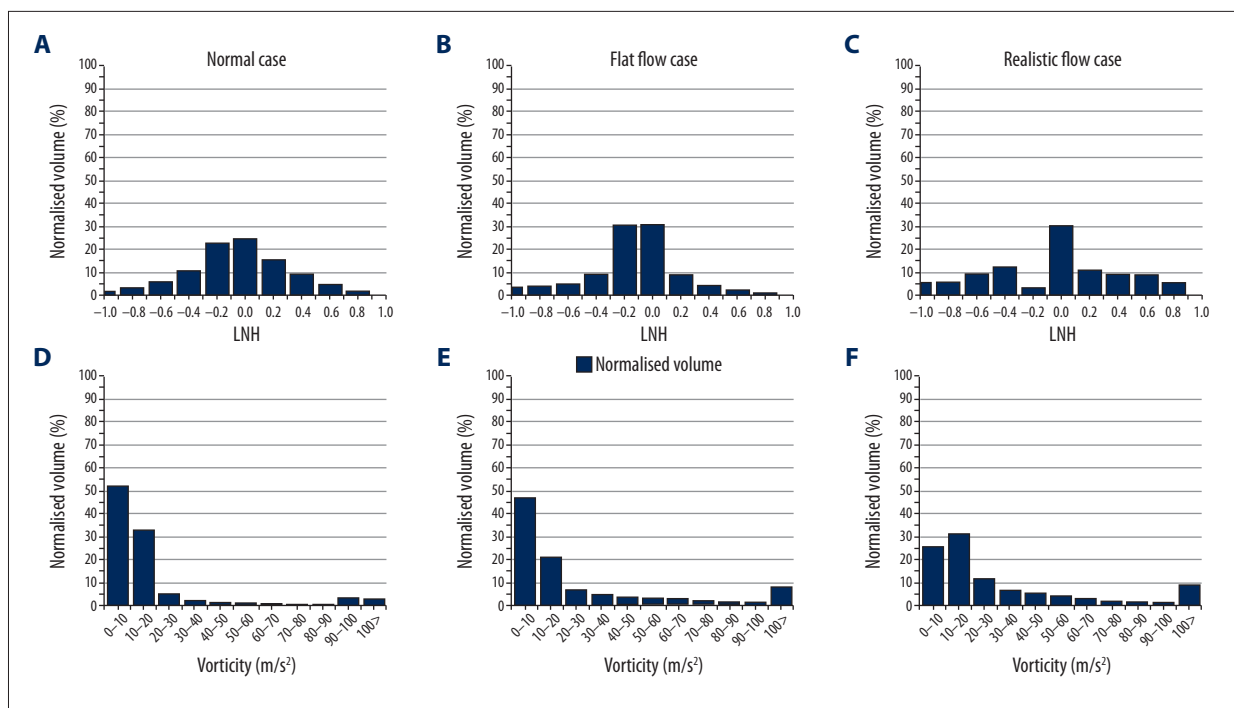
Figure 8. The distribution of LNH in the whole domain of aorta for all cases considered. The width of the bar is 0.2 for LNH.
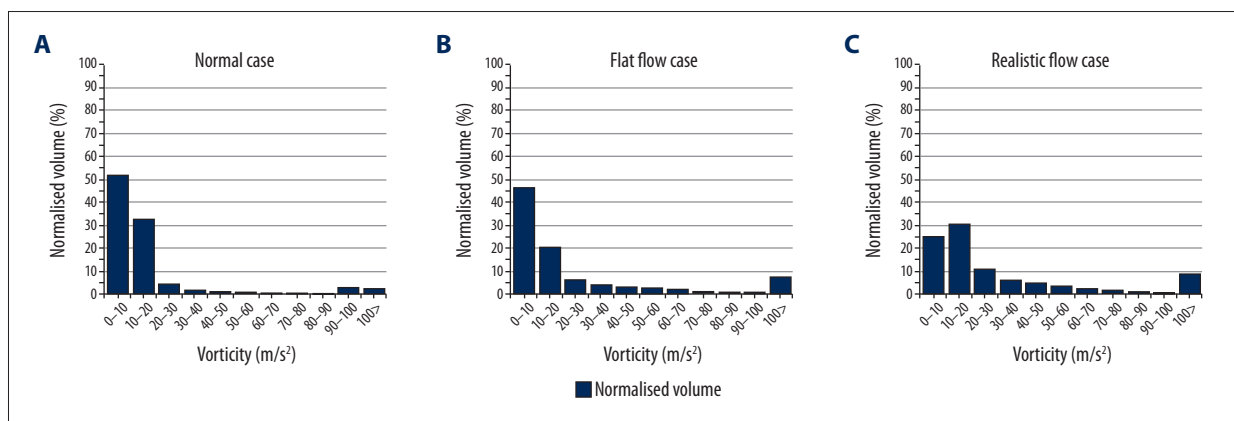

Figure 9. The distribution of blood vorticity in the whole domain of aorta for all cases considered. The width of the bar is 10 m/s^2 for blood vorticity.

To further illustrate the blood flow pattern under the 3 cases, the blood flow velocity vector in the aortic longitudinal plane is shown in Figure 4. It was seen that under normal case, no vortex was observed in the aortic blood flow, and the blood flow was smooth and orderly (Figure 4A). However, under LVAD support, the blood flow pattern in the ascending aorta was significantly disturbed by the LVAD outflow. The significantly lower velocity region (region a) was seen under both flat flow case and realistic flow case (normal case 0.30 m/s *vs.* flat flow case 0.05 m/s *vs.* 0.08 m/s). Moreover, under flat flow case, a vortex was found near the outer wall of the ascending aorta (region a), while under realistic flow case the vortex was eliminated. In addition, under flat flow case, the blood flow velocity near the aortic inner wall was significantly lower compared with that under both realistic flow case and normal case (region b). Similarly, blood velocity in the descending aorta under realistic flow case was significantly higher than that under flat flow case and normal case (normal case 0.1 m/s *vs.* flat flow case 0.14 m/s *vs.* realistic flow case 0.30 m/s) (region c).

The distribution of WSS

Figure 5 illustrates the distribution of WSS under 3 cases. Figure 5A and 5D illustrates the distribution of WSS under normal case. Figure 5B and 5E show the distribution of WSS under flat flow case. Figure 5C and 5F curved the distribution

of WSS under realistic flow case. It was seen that under LVAD support, the high WSS region was seen near the LVAD outflow cannula (region a and b). In addition, the peak value of WSS under flat flow case was significantly higher than that under both normal case and realistic flow case (normal case 0.92 Pa *vs.* flat flow case 7.39 Pa *vs.* realistic flow case 5.2 Pa). In contrast, the area of high WSS region under realistic flow case was larger than that under flat flow case.

Besides of the magnitude of WSS, the direction of WSS was also another important hemodynamic factor. Figure 6 showed the WSS vector obtained from 3 cases. It was seen that under normal case, the direction of WSS was more orderly than in the other 2 cases, and no disturbed WSS vector was observed. However, under LVAD support, the direction of WSS vector at the ascending aorta was significantly disturbed (region a), especially at the location where the jet of graft flow impinged (region c). Moreover, at the descending aorta, the WSS direction under flat flow case was obviously disturbed (region b). In contrast, the WSS at the descending aorta under realistic flow case was orderly (Figure 6C region b), which was similar with that under normal case.

The distribution of LNH and vorticity

Figure 7 illustrates the distribution of LNH in the aorta. Figure 7A illustrates the distribution of LNH under normal case. Figure 7B shows the distribution of LNH under flat flow case. Figure 7C illustrates the distribution of LNH under realistic flow case. It was seen that, under the normal case, the blood flow with clockwise rotational direction (LNH>0) predominated at the ascending aorta. In contrast, under LVAD support, there was a region at the proximal graft of LVAD outflow cannula, at where the rotational direction of the blood flow was changed from clockwise to counter-clockwise (region a). Among them, the area of the counter-clockwise region under realistic flow case was larger than that under flat flow case (Figure 7B region a *vs.* Figure 7C region a). In addition, the blood rotational direction at the descending aorta under flat flow case was disordered, while that under realistic flow case was more intact (region b).

A more detailed analysis is shown in Figures 8 and 9, showing it is possible to quantify the LNH and blood vorticity percentage distribution on the entire aorta. Thus, it enabled us to make a more detailed analysis of the results. It was seen that the percentage of clockwise blood (LNH >0.6) under realistic flow case was increased compared with that under both other cases. The percentage of slight counter-clockwise blood flow (–0.2< LNH <0) under realistic flow case was significantly reduced compared with that under both other cases. In addition, Figure 9 illustrates the blood vorticity percentage distribution on the entire aorta for the 3 cases considered. It was demonstrated that LVAD support could significantly enhance

the blood vorticity. The percentage of high blood vorticity (vorticity >20 m/s^2) under normal case was lower than 15%, while that under flat flow case and realistic flow case was higher than 35% and 55%, respectively. Moreover, the effect of flow pattern of LVAD outflow on the blood vorticity distribution was quite different from each other. In flat flow case, the percentage of blood vorticity, which was between 10~20 m/s^2, was significantly lower than that under normal case and realistic flow case (normal case: 32.6% *vs.* flat flow case: 20.8% *vs.* realistic flow case: 30.9%). In contrast, in realistic flow case, the percentage of blood vorticity, which ranged from 0 to 10 m/s^2, was obviously reduced compared with that under both other cases (normal case: 51.8% *vs.* flat flow case: 46.5% *vs.* 25.4%).

Discussion

LVADs have been widely applied in clinical practice. Although there are many studies on the effects of LVADs on aortic hemodynamic states, the LVAD outflow pattern was usually considered as the flat flow pattern [5–8]. However, our previous studies [15,23] confirmed that there was significant helical flow component in the LVAD outflow. The present study for the first time clarifies the hemodynamic effects of the helical flow component of the LVAD outflow on the aortic hemodynamic states.

Helical flow, as an important hemodynamic phenomenon, was firstly found in the aorta [24]. Although the helical flow was proven to have many advantages, its magnitude was thought to be attenuated along with the increase of the length of the vessel and cannula [25]. Because the LVAD outflow cannula is long, the helical component in the LVAD outflow is usually thought to be too small to influence the aortic hemodynamics. However, the results of our study show that obvious helical flow component was included in the LVAD outflow (Figure 3 region a). Hence, it was necessary to consider the effects of helical flow component of the LVAD outflow on the aortic hemodynamics. Under flat flow case, the symmetrically paired and counter-rotating helices, named Dean flow pattern, was found in the ascending aorta (Figure 3B). This was consistent with the flow pattern developing at a simple pipe bend. However, under realistic flow case, only single helical flow pattern was observed at the ascending aorta (Figure 3C), which was consistent with the physiological effects of helical flow in cardiovascular system. According to previous studies, the helical flow facilitates blood flow transport and suppress flow turbulence [26]. In terms of blood flow transport, Stonebridge demonstrated that compared with flat flow pattern, helical flow was more efficient and require less energy to drive blood through the arterial system [21]. Moreover, Morbiducci et al. reported that helical flow in the aorta was an optional blood transport process to avoid excessive energy dissipation, and

may contribute to achieving an efficient perfusion state [22]. This advantage also was shown in the present study. It was seen that the blood velocity at the descending aorta under realistic flow case was significantly higher than under flat flow case (Figure 4 region b). This means that the LVAD outflow, including helical flow component, can achieve more efficient blood flow transport, and then can reduce the energy dissipation, which might result in platelet activation and damage to erythrocytes [20]. In terms of suppression of turbulence, it was seen that under realistic flow case, the vortex, seen at the outer wall of the ascending aorta under flat flow case, was significantly attenuated (Figure 4 region a). In addition, the low blood velocity region, observed at the inner wall of the aortic arch, was eliminated by the helical flow component (Figure 4 region b). This means that the helical component of LVAD outflow can suppress flow turbulence resulting from the jetting flow of the LVAD.

WSS is a very important hemodynamic factor believed to have critical effects on regulating the structure and function of endotheliocytes. For instance, Hasin et al. reported that the endothelial function showed a significant and persistent decline under excessive WSS condition [27]. Uzarski et al. reported that the excessive shear stress magnitude could elicit phenotypic changes relevant to their critical roles in thrombosis, hemostasis, and inflammation [28]. In our study, the WSS magnitude was found be significantly reduced under realistic flow case (region c), while the area of relatively high WSS was also enlarged under realistic flow case. These changes were consistent with the physiological mean of helical flow. For instance, Ha et al. reported that the helical flow might lead to relative uniformity of wall shear stress. Therefore, enhancing the helical flow strength might have a benefit to reduce the peak value of WSS and to protect the function of endotheliocytes near the graft of the LVAD outflow cannula from dysfunction.

In addition to the magnitude of WSS, the direction of WSS was also an important factor. Peiffer demonstrated that the directionality of the wall shear stresses was a key factor that regulated the endothelial mechanotransducers and downstream signaling pathways [29]. Similarly, Wang demonstrated that the direction of hemodynamic stresses could alter the balance of pro- and anti-atherosclerotic signals within endothelial cells [30]. In our study, the direction of WSS was found to be significantly changed by LVAD support (Figure 5). Under normal case, the direction of WSS was consistent with each other, and no disturbed WSS was seen. Under LVAD support, the WSS near the graft of the LVAD outlet cannula was significantly disturbed by the jetting flow from the LVAD (region a and c). This change might result in dysfunction of endothelial cells near the graft of the cannula, which should receive more attention in clinical practice. Moreover, the situation of the direction of WSS at the descending aorta was totally different between flat flow case and realistic flow case (region b). Under the realistic flow case, the direction of WSS was more orderly and was similar to that in the normal case. However, the direction of WSS under flat flow case was severely disordered; therefore, endothelial cell function might be more severely impaired by the flat flow case.

Traditional LVAD design usually modifies the geometry of the impeller and diffuser to eliminate the helical flow to improve the LVAD efficiency. However, our results show that the helical flow component enhances blood transport efficiency, eliminating the stagnant flow zone, reducing the peak value of WSS, and providing a more orderly WSS direction. Hence, it might be a novel design aim to maintain appropriate helical flow strength in the LVAD outflow to improve the physiological benefit of LVADs. In addition, the combination of the novel LVAD design and the development of the technology for treatment of cardiovascular disease [31,32] might reduce mortality and improve the quality of life.

Limitations

In this study, the geometric model was reconstructed according to 1 patient's data. As the aim of this study was to clarify the potential physiological benefit from the helical flow of LVAD rather than determining the optimal level of the LVAD helical flow, we thought that 1 patient's data was enough for this study. The changes in the geometric size of the aorta and the blood boundary condition were confirmed to significantly affect the blood pattern in the aorta. Hence, there is a need for further studies in which the differences of geometric characteristics of the aorta and the variation on the blood boundary condition are obtained from different patients.

The static CFD simulations were conducted to clarify the aortic hemodynamic differences between flat flow condition, normal condition, and realistic flow condition. Although the transient boundary condition was considered as more accurate for hemodynamic study, the steady-state CFD simulations are still widely employed to study the aortic hemodynamics [33,34]. Hence, the steady-state CFD simulations also could provide much useful information for investigators. This study focused on the aortic hemodynamic changes resulting from the flat flow condition and helical flow condition. Hence, the steady-state CFD simulation could provide important hemodynamic information for researchers.

In this study, the static pressure condition was used as the outlet boundary condition, and the aorta was assumed to be a rigid wall in which the blood flow pattern is governed by the pressure gradient. Hence, the static pressure condition was confirmed to have little effect on the accuracy of the results.

This work is licensed under Creative Common Attribution-NonCommercial-NoDerivatives 4.0 International (CC BY-NC-ND 4.0)

878

Indexed in: [Current Contents/Clinical Medicine] [SCI Expanded] [ISI Alerting System]
[ISI Journals Master List] [Index Medicus/MEDLINE] [EMBASE/Excerpta Medica]
[Chemical Abstracts/CAS]

Conclusions

To evaluate the effect of helical flow component of LVAD outflow on the aortic hemodynamics, 3 cases (normal case, flat flow case, and realistic flow case) were studied by using the CFD approach. The results demonstrated that the helical flow component in LVAD outflow significantly improved the aortic hemodynamics. Compared with flat flow case, the helical flow eliminated the vortex near the outer wall of the aorta and improved the blood flow transport (normal case 0.1 m/s *vs.* flat flow case 0.14 m/s *vs.* realistic flow case 0.30 m/s) at the descending aorta. Moreover, the helical flow was confirmed to even the distribution of WSS, to reduce the peak value of WSS (normal case 0.92 Pa *vs.* flat flow case 7.39 Pa *vs.* realistic flow case 5.2 Pa), and to maintain a more orderly WSS direction. In short, the helical flow component of LVAD outflow had significant advantages for improving aortic hemodynamic stability. Our study provides novel insights into LVAD optimization for investigators.

References:

1. Mulloy DP, Bhamidipati CM, Stone ML et al: Orthotopic heart transplant versus left ventricular assist device: A national comparison of cost and survival. J Thorac Cardiovasc Surg, 2013; 145(2): 566–73

2. Slaughter MS, Rogers JG, Milano CA et al: Advanced heart failure treated with continuous-flow left ventricular assist device. N Engl J Med, 2009; 361(23): 2241–51

3. Rogers JG, Pagani FD, Tatooles AJ et al: Intrapericardial left ventricular assist device for advanced heart failure. N Engl J Med, 2017; 376(5): 451–60

4. Karmonik C, Partovi S, Loebe M et al: Influence of LVAD cannula outflow tract location on hemodynamics in the ascending aorta: A patient-specific computational fluid dynamics approach. Asaio J, 2012; 58(6): 562–67

5. Karmonik C, Partovi S, Schmack B et al: Comparison of hemodynamics in the ascending aorta between pulsatile and continuous flow left ventricular assist devices using computational fluid dynamics based on computed tomography images. Artif Organs, 2014; 38(2): 142–48

6. Caruso MV, Gramigna V, Rossi M et al: A computational fluid dynamics comparison between different outflow graft anastomosis locations of Left Ventricular Assist Device (LVAD) in a patient-specific aortic model. Int J Numer Method Biomed Eng, 2015; 31(2)

7. Yang N, Deutsch S, Paterson EG et al: Numerical study of blood flow at the end-to-side anastomosis of a left ventricular assist device for adult patients. J Biomech Eng, 2009; 131(11): 111005

8. Zhang Y, Gao B, Yu C: The hemodynamic effects of the LVAD outflow cannula location on the thrombi distribution in the aorta: A primary numerical study. Comput Methods Programs Biomed, 2016; 133: 217–27

9. Gu K, Gao B, Chang Y et al: Pulsatile support mode of BJUT-II ventricular assist device (VAD) has better hemodynamic effects on the aorta than constant speed mode: a primary numerical study. Med Sci Monit, 2016; 22: 2284–94

10. Kilner PJ, Yang GZ, Mohiaddin RH et al: Helical and retrograde secondary flow patterns in the aortic arch studied by three-directional magnetic resonance velocity mapping. Circulation, 1993; 88(5 Pt 1): 2235–47

11. Zabielski L, Mestel AJ: Steady flow in a helically symmetric pipe. J Fluid Mech, 1998; 370: 297–320

12. Frydrychowicz A, Markl M, Hirtler D et al: Aortic hemodynamics in patients with and without repair of aortic coarctation: *In vivo* analysis by 4D flow-sensitive magnetic resonance imaging. Invest Radiol, 2011; 46(5): 317–25

13. Frazin LJ, Vonesh MJ, Chandran KB et al: Confirmation and initial documentation of thoracic and abdominal aortic helical flow. An ultrasound study. ASAIO J, 1996; 42(6): 951–56

14. Coppola G, Caro C: Oxygen mass transfer in a model three-dimensional artery. J R Soc Interface, 2008; 5(26): 1067–75

15. Zhang Q, Gao B, Chang Y: The study on hemodynamic effect of series type LVAD on aortic blood flow pattern: A primary numerical study. BioMed Eng OnLine, 2016; 15(Suppl. 2): 163

16. Chang Y, Gao B: Modeling and Identification of an Intra-Aorta Pump. ASAIO J, 2010; 56(6): 504–9

17. Kousera CA, Wood NB, Seed WA et al: A numerical study of aortic flow stability and comparison with *in vivo* flow measurements. J Biomech Eng, 2013; 135(1): 011003

18. Tan FPP, Torii R, Borghi A et al: Fluid-structure interaction analysis of wall stress and flow patterns in a thoracic aortic aneurysm. International journal of applied mechanics, 2009; 1: 179–99

19. Singh SD, Xu XY, Wood NB et al: Aortic flow patterns before and after personalised external aortic root support implantation in Marfan patients. J Biomech, 2016; 49(1): 100–11

20. Vahidkhah K, Cordasco D, Abbasi M et al: Flow-induced damage to blood cells in aortic valve stenosis. Ann Biomed Eng, 2016; 44(9): 2724–36

21. Stonebridge PA, Brophy CM. Spiral laminar flow in arteries? Lancet, 1991; 338: 1360–61

22. Morbiducci U, Ponzini T, Rizzo G et al: Mechanistic insight into the physiological relevance of helical blood flow in the human aorta: An *in vivo* study. Biomech Model Mechanobiol, 2011; 10: 339–55

23. Zhang Q, Gao B, Chang Y: Effect of different rotational directions of BJUT-II VAD on aortic swirling flow characteristics: a primary computational fluid dynamics study. Med Sci Monit, 2016; 22: 2576–88

24. Frazin LJ, Lanza G, Vonesh M et al: Functional chiral asymmetry in descending thoracic aorta. Circulation, 1990; 82: 1985–94

25. Liu X, Pu F, Fan Y et al: A numerical study on the flow of blood and the transport of LDL in the human aorta: the physiological significance of the helical flow in the aortic arch. Am J Physiol Heart Circ Physiol, 2009; 297(1): H163–70

26. Liu X, Sun A, Fan Y et al: Physiological significance of helical flow in the arterial system and its potential clinical applications. Ann Biomed Eng, 2015; 43(1): 3–15

27. Hasin T, Matsuzawa Y, Guddeti RR et al. Attenuation in peripheral endothelial function after continuous flow left ventricular assist device therapy is associated with cardiovascular adverse events. Circ J. 2015, 79(4): 770–77

28. Uzarski JS, Scott EW, McFetridge PS: Adaptation of endothelial cells to physiologically-modeled, variable shear stress. PLoS One, 2013; 8(2): e57004

29. Peiffer V, Sherwin SJ, Weinberg PD: Computation in the rabbit aorta of a new metric the transverse walls shear stress to quantify the multidirectional character of disturbed blood flow. J Biomech, 2013; 46: 2651–58

30. Wang C, Baker BM, Chen CS et al: Schwartz. Endothelial cell sensing of flow direction. Arterioscler Thromb Vasc Biol, 2013; 33: 2130–36

31. Sarsam S, Kaspar G, David S et al: Early detection of subclinical aortic valve endocarditis with the CardioMEMS heart failure system. Am J Case Rep, 2017; 18: 665–68

32. Li K, Xue Q, Liu M et al: Noninvasive cardiac quantum spectrum technology effectively detects myocardial ischemia. Med Sci Monit, 2016; 22: 2235–42

33. Liu X, Pu F, Fan Y et al: A numerical study on the flow of blood and the transport of LDL in the human aorta: the physiological significance of the helical flow in the aortic arch. Am J Physiol Heart Circ Physiol, 2009; 297(1): H163–70

34. Liu X, Fan Y, Deng X: Effect of spiral flow on the transport of oxygen in the aorta: A numerical study. Ann Biomed Eng, 2010; 38(3): 917–26